Materials Characterization 142 (2018) 540–549

Contents lists available at ScienceDirect

Materials Characterization

journal homepage: www.elsevier.com/locate/matchar

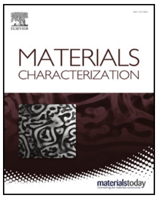

# TEM study the corrosion behavior of the low alloy steels developed for flue gas desulfurization system

Yinsheng He[a], Keun-Bong Yoo[a], Joong Cheul Park[b], Byung-Ho Lee[c], Jeong-Bong Yoon[d], Jung-Gu Kim[e], Keesam Shin[f,*]

[a] *Clean Power Generation Lab., KEPCO Research Institute, Daejeon 34056, Republic of Korea*
[b] *Analysis & Assessment Department, Research Institute of Industrial Science & Technology, Pohang 37673, Republic of Korea*
[c] *Sheet Products & Process Research Group, Technical Research Laboratories, POSCO, Pohang 37859, Republic of Korea*
[d] *College of Mechatronics, Changwon National University, Changwon 51140, Republic of Korea*
[e] *Department of Advanced Materials Science and Engineering, Sungkyunkwan University, Suwon 03063, Republic of Korea*
[f] *School of Nano & Advanced Materials Engineering, Changwon National University, Changwon 51140, Republic of Korea*

## ARTICLE INFO

*Keywords:*
Low alloy steels
Acid corrosion
Corrosion layers
Alloying effect
Cu particles
TEM

## ABSTRACT

This study investigated the corrosion behavior and underline mechanisms of low alloy steels with a minor addition of 0.4 wt% Cu, 0.2 wt% Ni, 0.1 wt% Sb and 0.05 wt% Co developed for a flue gas desulfurization (FGD) system. Corrosion tests were carried out in an aggressive solution of 16.9 vol% $H_2SO_4$ + 0.35 vol% HCl + Bal. $H_2O$ at 60 °C for up to 48 h. The experimental results revealed enrichment of the additional elements (Cu, Sb and Ni) in the corrosion layer, whose concentration increased with test time. As the concentrations of Cu increased, the crystallization and growth of the Cu particles (from several nm to 320 nm)) within the corrosion layer was accelerated. At the initial stage of the test, a continuous amorphous layer rich with the additional elements formed and covered the surface of the steel, which then gradually developed defects, pores and cracks, as the crystallization and growth of Cu particles with the elapse of time. The results indicated that the corrosion resistance of the low alloy steel depends on the existence form of Cu in the corrosion layer, i.e., as solute atoms or as nanoparticles strengthened the corrosion layer and increased corrosion resistance. As the coarsening of Cu particles weakened the corrosion layer and deteriorated the corrosion resistance.

## 1. Introduction

Low alloy steel with the minor alloying elements (< 0.3 wt%) Cu, Sb, Ni, Co, Cr, Nb and Ti) have excellent strength, corrosion resistance and welding properties at low cost. Optimizing the content of additives allows their wide application in various areas, such as weathering steel to resist atmospheric corrosion [1–4], ocean industrial steel to resist seawater corrosion [3, 5, 6], and even in the complex acid corrosion environment of the FGD system in coal-fired power plants to resist acid dew corrosion [7–10] and synthetic tab water system to resist aqueous corrosion [11]. Previous studies commonly indicated that the corrosion resistance of this type of steel is due to the formation of a dense corrosion layer that isolates the steel from the corrosive environment and inhibits further corrosion [1, 2, 10, 12–14].

In the past two decades, extensive work has been carried out in the investigation of the alloying effect on the corrosion layer and corrosion products by using various characterization techniques [15]: X-ray powder diffraction (XRD) [4, 16], Mossbauer spectroscopy [17], Raman spectroscopy [18], atomic force microscopy (AFM) [19] and a combination of X-ray photoelectron spectroscopy (XPS) with scanning electron microscopy (SEM) [6–9, 11, 20–31]. For example, the formation of the additional "*M*-oxide" (*M* as the additives of alloying elements) within the "dense corrosion layer" is the main mechanism related to the improvement of corrosion resistance. The type of the "*M*-oxide" is determined by a chemical formula applied to the XPS results by matching the binding energy with the standard value. However, some oxides have similar binding energies, for example, the Cu, CuO and $Cu_2O$ own the binding energy of 932.7 eV, 932.5 eV and 933.4 eV, respectively, which make them hard to distinguish. The "dense corrosion layer" is characterized by surface and cross-sectional observation using SEM, in which the samples are prepared by traditional methods, including cutting, mounting and polishing procedures, which may cause the corrosion layer to damage its original morphology. Furthermore, enrichment of the additional elements on the surface is characterized by the energy dispersive spectrometer (EDS) and electron probe microanalysis (EPMA) [7, 9, 25–27, 29], but the usefulness of these

---

* Corresponding author.
*E-mail addresses:* keesamgg@gmail.com, keesam@changwon.ac.kr (K. Shin).

https://doi.org/10.1016/j.matchar.2018.06.007
Received 29 December 2017; Received in revised form 4 June 2018; Accepted 4 June 2018

mechanisms for enrichment is under debate [7, 32]. Understanding the corrosion mechanism of the low alloy steels is important, since it give the significant role of guideline on the design and modify of the steels with optimized composition to give better properties upon various complex corrosion environment.

Detailed TEM analyses of the corrosion layer and corrosion products have rarely been reported [3, 4]. For example [3], the phases of the corrosion products were determined by selective area diffraction pattern (SADP) analysis in TEM. In this analysis, samples were prepared from the corrosion products using the nano-powder procedures (grinding, suspension in ethyl alcohol and floating with a TEM grid). Furthermore, the role of the corrosion products in the corrosion layer has not been clarified, since most of the reported literatures focused on the study of the corrosion layer of long-term field-serviced coupons [3, 23, 33]. The evolution of the corrosion products during tests has yet to be determined.

In this study, we focused on the study of corrosion mechanism which involved the evolution of corrosion products within the corrosion layer. We tested the low alloy steels (containing Cu, Sb and Ni) developed for the FGD system in an accelerated corrosion environment [7, 25, 34]. After the test, the corrosion products and the corrosion layer that formed were microscopically analyzed using SEM, focused ion beam (FIB) and TEM for 1) the morphologies and distribution of the microstructural features with the corresponding chemical composition; 2) microstructural evolution; and 3) understanding the alloying effect.

## 2. Experimental Procedures

### *2.1. Materials and Corrosion Test*

Recently developed and commercialized (by POSCO) low alloy steels called ANCOR-HS and ANCOR-H were used [34]. As shown in Table 1, the chemical composition (in wt%) of the studied steels contained the basic element 0.07C-0.4Si-1.0Mn-0.01P-0.002S, and the alloy 0.4Cu-0.2Ni-0.05Co with/without of 0.1Sb. Square plates ($1 \times 1 \times 0.3\ \mathrm{cm}^3$) were polished with 800 grit sand paper, cleaned with distilled water followed by ethanol and hot-air, and then loaded into 1000 ml of the “modified green death solution” (MGD, $H_2SO_4$- 16.9 vol% + HCl- 0.35 vol% + $H_2O$- balance) [25] as quickly as possible to minimize the exposure of the surface to the atmosphere. The MGD solution is the best representative of the accelerated corrosion environment in Korean FGD facilities. The immersion time intervals and durations are listed in Table 2. In addition, a blank specimen (without any additional elements, Table 1) was also used in a test of only 10 min.

### *2.2. Microstructural Analysis*

The microstructural characterization of the surface and cross-section was done by utilizing the SEM and TEM. After the test, the surface of the tested pieces was studied using the SEM and EDS. A cross-sectional view of the corrosion layer was accomplished by directly cutting the corrosion layer using FIB, so that the original morphology of the corrosion layer was retained. A final FIB thinning was used to fabricate the electron transparent thin foil for TEM study. Table 2 lists the specimens used for the TEM study. In addition, the powders dropped from the specimens within the solution were collected by centrifugation; they were then dried and finally studied by SEM and TEM.

SEM studies were carried out on a JSM-5610 equipped with an Oxford-Inca EDS system. Cross-sectional TEM (X-TEM) sampling was performed on an SIM3050 FIB using the traditional lift-off process; prior to the FIB work, a carbon film (or Pt) was deposited on the surface of the samples. (S)TEM, HRTEM observations and EDS analyses were performed on a JEM-2100F field emission microscope equipped with the Oxford Inca EDS system. Analyses of the selected area diffraction patterns (SADP) were carried out utilizing the JEMS and Gatan Digital Microscope software.

## 3. Results and Discussion

Both the HS and H specimens were investigated, as shown in Table 2. The results of the corrosion products in the corrosion layer of the two specimens were similar; the detailed explanation is shown in terms of the HS specimens. The H specimens, particularly the Sb effect in particular, will be discussed below.

### *3.1. Corrosion Behavior of the Blank Specimen*

Fig. 1a shows the surface morphologies of the blank specimen after it was tested for 10 min. The results suggest that the surface was severely damaged and had sustained micro-sized cracks and pores. Fig. 1b shows a cross-sectional view, which clearly shows the morphology of micro-sized interface cracks (along the interface), pores and cracks (vertical to the interface) in the corrosion layer. Even in the specimen that was tested for only 10 min, the thickness of the corrosion layer formed was up to ~12 μm and contained obvious porous structures. It also seemed that the corrosion layer could easily fall-off of the matrix due to the interface crack. When the blank specimen was loaded into the MGD solution, an immediate observation was the dissolution of the Fe matrix and the drop-off of the corrosion layer with the emission of gas ($H_2$) from the solution. Fig. 1c shows the X-TEM image of the corrosion layer, in which enrichment of Fe, S and O was observed in the TEM/EDS analysis (inset table). The corresponding SADP (Fig. 1d) shows that the corrosion layer is an amorphous state, which agrees with the results of Panossian, et al. [13], indicating that the corrosion layer might be the precursor of the $FeSO_4$ and FeOOH corrosion products. The presence of the amorphous corrosion layer may be due to the solubility of $FeSO_4$ and FeOOH in the acid solution.

### *3.2. Corrosion Behavior of the HS Specimen*

#### *3.2.1. SEM Analysis*

Before the test, the surface of the specimens was full of scratches (SEM result not shown here) introduced by the mechanical polishing. After the test, the surfaces were observed using SEM; some of the typical changes in surface morphologies are shown in Fig. 2. Up to 30 min, the scratches on the surface are faint (Fig. 2a1). At 30 min and 3 h, some pits were observed, but just barely; in addition, it seemed that a dense corrosion layer covered the surfaces, as shown in Fig. 2b1. A higher magnification view of the surface shows that the surface was enriched with nano-sized particles (Fig. 2b2). When the time increased to 6 h (Fig. 2c1 and c2), a very dense layer with a dispersion of nano-sized particles covered the surface. As the test time increased to 12 h,

**Table 1**
Chemical composition of the specimens used in this study (wt%/at.%).

| Specimens | Basic | | | | | | Additional elements | | | |
|---|---|---|---|---|---|---|---|---|---|---|
| | C | Si | Mn | P | S | Fe | Cu | Ni | Co | Sb |
| Blank | 0.07/0.32 | 0.25/0.50 | 0.2/0.20 | 0.01/0.02 | 0.01/0.02 | 99.46/98.94 | – | – | – | – |
| ANCOR-H | 0.07/0.32 | 0.4/0.79 | 1.0/1.01 | 0.01/0.02 | 0.002/0.003 | 97.77/97.22 | 0.4/0.35 | 0.2/0.19 | 0.05/0.05 | – |
| ANCOR-HS | DITTO | | | | | | | | | 0.1/0.05 |